



# Effects of predeformation and semi-solid processing on microstructure and mechanical properties of Cr–V–Mo steel

Yi Meng\*, Sumio Sugiyama, Mehdi Soltanpour, Jun Yanagimoto

*Institute of Industrial Science, The University of Tokyo, Komaba 4-6-1, Meguro, Tokyo 153-8505, Japan*

## ARTICLE INFO

### Article history:

Received 13 July 2012

Accepted 24 September 2012

Available online 2 October 2012

### Keywords:

Semi-solid forming

RAP

Tool steel

Refinement

Mechanical properties

## ABSTRACT

An energy-efficient process route for manufacturing machine tools and dies of high quality was proposed based on recrystallization and partial melting (RAP) method and semi-solid forming technology. To verify its feasibility, the effects of parameters such as predeformation, heating rate, and holding time on the microstructure and mechanical properties of cast Cr–V–Mo steel were studied experimentally. Recrystallization, austenitization, grain growth and partial melting occur during heating of predeformed cast billet. These behaviors refine the microstructure and improve the mechanical properties. The refinement of microstructure and improvement of mechanical properties become more significant, when RAP is conducted with larger predeformation (50%), higher heating rate (50 °C/s) and shorter isothermal holding time (20 s).

© 2012 Elsevier B.V. All rights reserved.

## 1. Introduction

To promote the wide utilization of tool steel in machine tools and dies, excellent mechanical properties, such as hardness, toughness, strength, and corrosion resistance are required. Roberts et al. (1998) pointed out that a fine-grained martensite matrix with a uniform carbide distribution is the guarantee of high-quality tool steel products. In manufacturing, the refinement of the microstructure and the homogeneous distribution of carbides and nitrides are indispensable.

The conventional manufacturing method for tool steel is multipass hot rolling with the subsequent heat treatments. After being held isothermally at high temperatures for about 1 day to induce homogenization, the cast stock is deformed through nearly 20 passes of hot rolling. The large strain accumulated in hot rolling induces the recrystallization of the coarse dendritic cast structure, as demonstrated by Barani et al. (2006). Martensite transformation and precipitation hardening are achieved by subsequent heat treatments. The 1 day preheating and multipass hot forming consumes large amounts of energy and time and results in a long process chain for the manufacture of products. Environmental consciousness and the demand for better products are fueling the development of an improved route with a shorter process chain and lower energy consumption that can replace the conventional one.

Semi-solid forming technology has a long history of investigation, following the discovery by Spencer et al. (1972) of the rheological properties of semi-solid metals. The characteristic microstructure of semi-solid metals, consisting of equiaxed solid particles in a liquid matrix, results in the adjustable viscosity and fluidity of the metal (Flemings, 1991), hence affecting the forming behavior (Li et al., 2005), and affects the distribution of alloying elements. Püttgen et al. (2007) showed the variation in the chemical compositions of the solid and liquid phases, and such composition variation still remains in metals rapidly cooled from a semi-solid state.

To fabricate semi-solid ferrous metal billets with a fine-grained spherical microstructure, various fabrication methods have been used. Hirt et al. (2005) employed the cooling slope method proposed by Adachi et al. (1996) and Haga et al. (1998) to manufacture thixoformable semi-solid tool steels. Song et al. (2008) utilized electromagnetic stirring technology raised by Griffiths and McCartney (1996) and rheorolling to produce stainless steel strips. These methods use special equipment such as electromagnetic stirring machine, which lead to stringent requirements for the material of tools in contact with the molten ferrous metal. By considering the simplicity of equipment and the low degradation of tools, the strain-induced melt activation (SIMA) route discovered by Young et al. (1983) and the recrystallization and partial melting (RAP) route invented by Kirkwood et al. (1991) appear to be preferable methods of fabricating ferrous metal billets with an equiaxed spherical microstructure. Both methods involve the partial melting of the recrystallized metal slurry (Atkinson and Rassili, 2010). The capabilities of the RAP method for fabricating spherical tool steel

\* Corresponding author. Tel.: +81 3 5452 6204; fax: +81 3 5452 6204.

E-mail address: [meng@iis.u-tokyo.ac.jp](mailto:meng@iis.u-tokyo.ac.jp) (Y. Meng).

**Table 1**  
Chemical composition of the starting material (wt%).

C	Si	Mn	P	S	Cu	Ni	Cr	V	Mo	Fe
0.36	0.94	0.47	0.014	0.003	0.09	0.06	5.26	0.8	1.2	Bal.

slurries has been investigated and verified by Meng et al. (2012). Besides these methods, the inverse peritectic induced spheroidization of some steel can lead to spheroidization as reported by Li et al. (2008).

In consideration of the spherical microstructure and flexible forming property of metals in a semi-solid state, the RAP method is applied as a critical part to improve the conventional route and shorten the process chain of tool steel products manufacturing. The refinement of the microstructure and the homogeneous distribution of alloying elements are crucial for realizing such a short process, which can be considered as “semi-solid thermomechanical processing”. After being annealed for 3 h, cast billet is subjected to RAP processing including warm deformation and partially melting. Subsequently, the RAP processed billet is thixodeformed to the desired shape directly in a semi-solid state. A following single pass hot forming can be conducted selectively to promote further grain refinement by recrystallization. Adjustable heat treatment and machining in the subsequent stage complete the fabrication of products with the desired geometries and mechanical properties. What is important to accomplish in this route is to determine how many grains of cast billet are refined by RAP and the uniformity of the alloying elements distribution that can be achieved.

With the aim of investigating and verifying the feasibility of manufacturing tool steel products with excellent mechanical properties using improved route, RAP, which is a critical part of this route, was investigated. The evolution of the microstructure and the distribution of alloying elements and their carbides and nitrides in cast Cr–V–Mo steel (JIS SKD61, AISI H13, DIN 1.2344) during RAP were clarified experimentally. A series of tensile tests were carried out to study and quantify the mechanical properties of cast Cr–V–Mo steel before and after RAP treatment.

## 2. Experimental procedure

### 2.1. Materials

Commercial rolled SKD61 hot-working steel was cast into a cast block as the starting material. Its chemical composition is shown

in Table 1. According to its cooling curve, the solidus and liquidus temperatures of the starting material are 1318 °C and 1489 °C, respectively. To improve the plasticity and homogeneity, the cast block was annealed at 850 °C for 3 h and then machined into rectangular specimens of 50 mm length, 20 mm width, and 10 mm height.

### 2.2. RAP experiment

RAP entails two working steps: warm predeformation and partial melting. Warm predeformation was conducted by upsetting using a multistage hot-compression testing machine. The experimental setup and the dimensions of the die are shown in Fig. 1. An induction coil was installed on a frame located in the operation zone of the testing machine. The specimen was fixed at the center of the induction coil by two horizontal springs connecting the specimen to the frame. A pair of ceramic flat dies gripped the specimen in the vertical direction. A thermocouple was welded onto the specimen to measure and control its temperature. The movement of both the upper die and the frame was controlled by a computer system. As the specimen and induction coil were both fixed on the frame, computer system ensured that the geometric centers of the specimen and the pair of dies were coincident throughout the experiment. The springs fixed at both ends of the specimen protected it from being bent during deformation. Upsetting experiments with 25% and 50% reductions at 300 °C were carried out at a constant strain rate of 1/s.

The same equipment was employed in the partial melting experiment. Predeformed specimens were partially melted by various heating strategies. Subsequently, rapidly water cooling was conducted to freeze the microstructures. To prevent the specimens from oxidation at high temperatures, nitrogen was used as the inert atmosphere.

### 2.3. Microstructural observation and measurement of mechanical properties

After being polished and etched in 10% nitric acid/alcohol solution, the microstructure of the specimens were observed using a

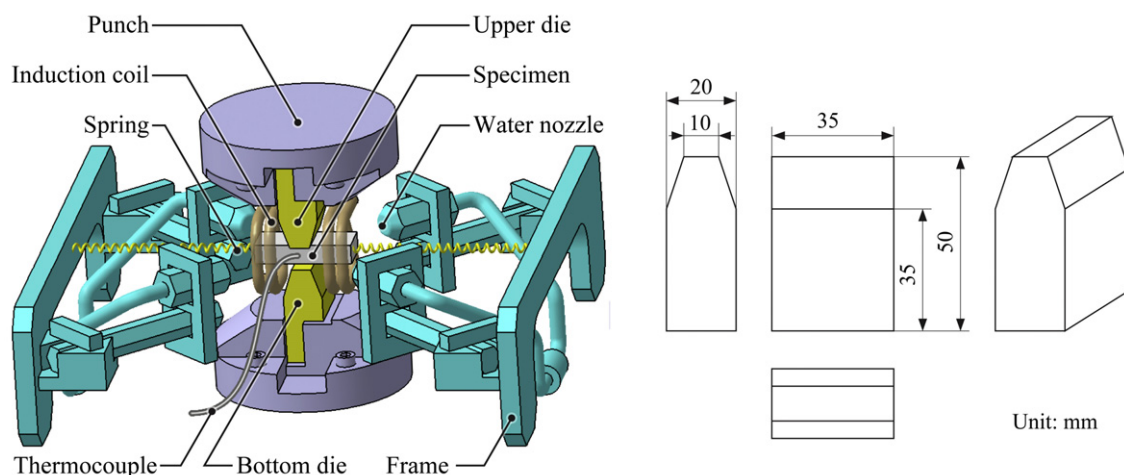


**Fig. 1.** Schematic diagram of upsetting experimental setup (left) and dimensions of die (right).

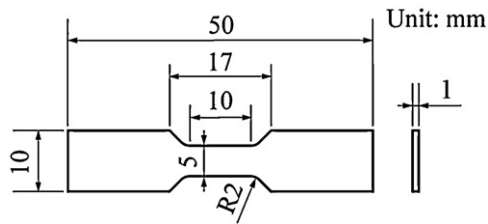


Fig. 2. Dimensions of tensile specimen.

Keyence VH-5500 optical microscope. Specimens processed under various experimental conditions were machined into tensile specimens with the dimensions shown in Fig. 2. A tensile test was carried out using a Shimadzu AGS-50kNG tensile tester at room temperature with a cross-head speed of 1 mm/s. The fracture surfaces were observed using a JEOL JSM-5600 scanning electron microscope.

### 3. Results and discussion

#### 3.1. Starting material

Fig. 3 shows an optical micrograph of starting material. A coarse casting structure with a large grain size of about  $200\ \mu\text{m}$  was observed. The result of the SEM-EDS mapping shown in Fig. 4 indicates an inhomogeneous distribution of carbides in the cast Cr–V–Mo steel block. Alloying elements such as C, Si, and Mo are condensed in interdendritic regions. This phenomenon is due to the microsegregation of impurities and alloying elements during the dendritic growth mode solidification of cast steel (Metals Handbook, 1998).

#### 3.2. Microstructural evolution during RAP

Optical micrographs of the center area of the specimens compressed by 50% height reduction at  $300\ ^\circ\text{C}$  under various heating conditions are shown in Fig. 5.

As shown in Fig. 5b, ferrite grains of the predeformed specimen were distorted but without obvious change in grain size. Carbides in interdendritic regions extended in the direction perpendicular to the upsetting direction. As  $300\ ^\circ\text{C}$  is lower than the recrystallization

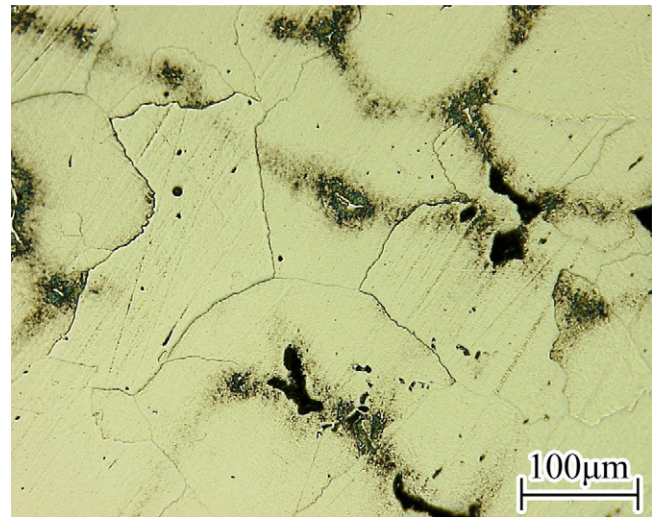


Fig. 3. Optical micrograph of annealed cast Cr–V–Mo steel at room temperature.

temperature, no recrystallization occurred. According to our previous study (Meng et al., 2012), warm predeformation increases the density of dislocations along grain boundaries, and causes the accumulation of deformation energy. Once the temperature exceeds recrystallization temperature of the cast Cr–V–Mo steel of about  $870\ ^\circ\text{C}$ , recrystallization occurs and resulted in new formed small grains. As shown in Fig. 5c, a certain number of smaller grains of about  $20\ \mu\text{m}$  exist among the former distorted grains at  $900\ ^\circ\text{C}$ . During recrystallization, carbides in the interdendritic regions provide nucleation sites and inhibit grain growth. Grains near carbides are smaller than the grains in other regions. As the temperature exceeds the austenitization temperature, austenitization and recrystallization occur simultaneously. Carbides dissolve into austenite grains, resulting in a one-phase austenite structure, as shown in Fig. 5d. In further heating, the growth of austenite grains occurs to reduce internal surface energy and results in a one-phase austenite structure with larger at  $1250\ ^\circ\text{C}$ , as shown in Fig. 5e. When the temperature exceeds the solidus temperature, partial melting initially takes place on grain boundaries. Liquid phase penetrates all the grain boundaries and forms an interconnected

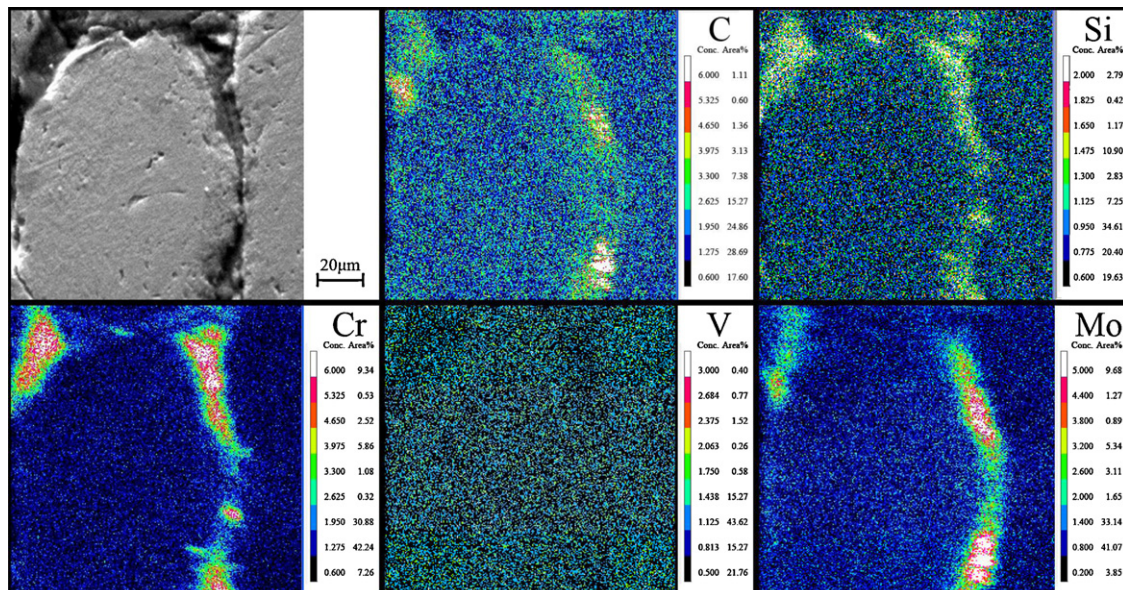


Fig. 4. SEM-EDS mapping of cast Cr–V–Mo steel at room temperature.

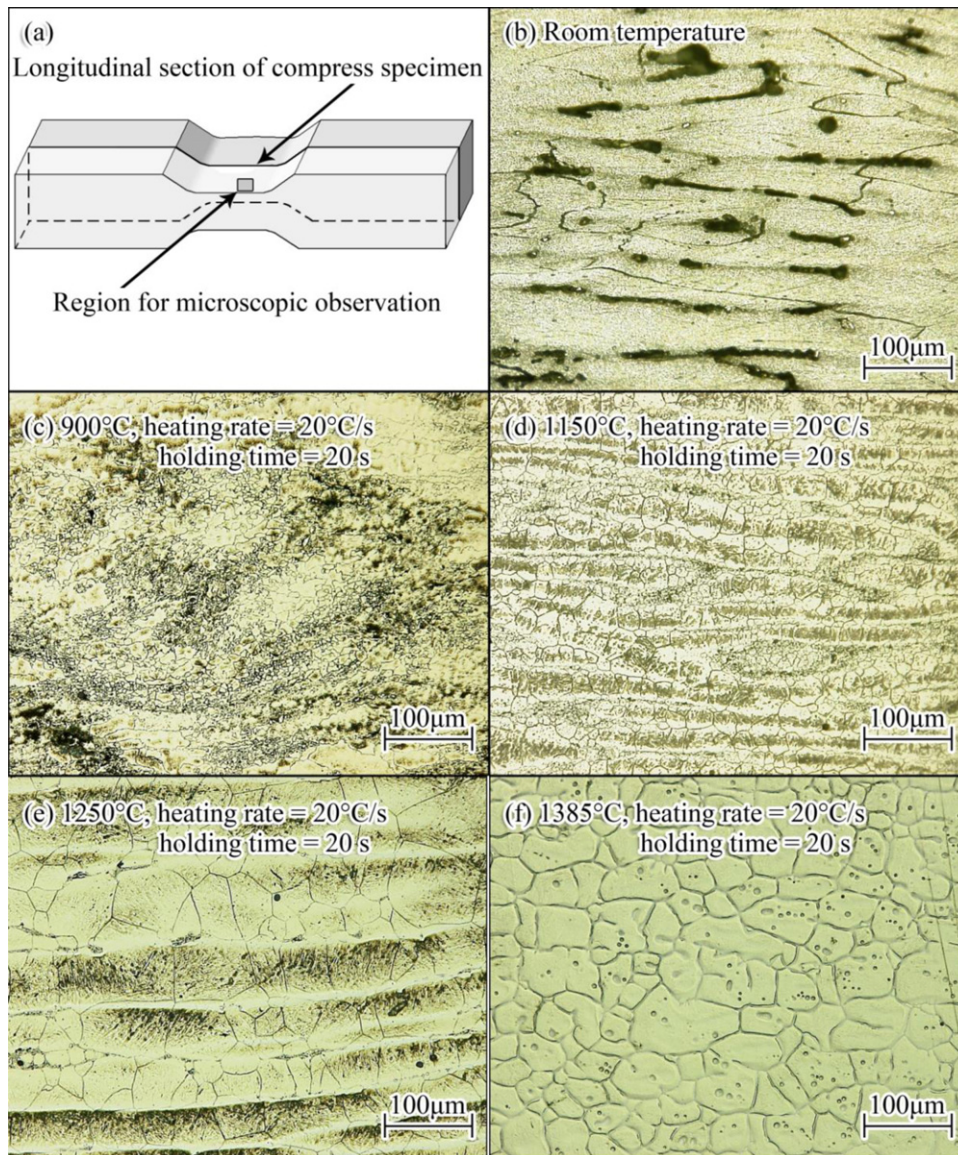


Fig. 5. Optical micrographs of specimen predeformed with 50% height reduction and then processed under various heating conditions.

liquid network. Solid particles tend to be spherical to reduce their surface energy. A microstructure with discrete spherical solid particles in a liquid matrix is obtained at 1385 °C, as shown in Fig. 5f. The entrapped liquid drops inside solid particles are resulted from the alloying elements entrapped in grains during the growth and combination of austenite grains.

The SEM-EPMA mapping of the RAP-processed specimen predeformed with a 50% height reduction is shown in Fig. 6. Alloying elements are mainly located in the former liquid networks surrounding the solid particles. This phenomenon is attributed to partial melting of the regions rich in alloying elements, such as grain boundaries, and diffusion of alloying element from discrete solid particles to interconnected liquid networks with further melting, as reported by Püttgen et al. (2005). The distribution of carbides in the RAP-processed specimen is more uniform than that of starting material.

### 3.3. Effect of predeformation on microstructure

Optical micrographs of the specimens predeformed with a 25% height reduction at 300 °C and quenched at various temperatures

are shown in Fig. 7. As shown in Fig. 7a, smaller predeformation distorted the ferrite grains slightly and retained less deformation energy in the deformed specimen. Less recrystallization occurs in heating, leading to a nonfine recrystallized structure with a large number of elongated grains at 900 °C and an austenite structure with coarse grains (about 140 µm) at 1250 °C, as shown in Fig. 7b and c, respectively.

The dissolution of alloying elements in the specimen is affected by the predeformation. The deformation energy retained in the slightly distorted specimen does not provide sufficient activation energy for the diffusion of alloying elements. In an insufficiently recrystallized structure, the interfaces of carbides and austenite grains are smaller than those in a sufficiently recrystallized structure. Carbides located in interdendritic regions do not dissolve uniformly, and some carbides even exist at 1250 °C, as shown in Fig. 7c. These regions with undissolved carbides transform to a large amount of the liquid phase and can be observed as clusters of smaller grains in a quenched specimen. At 1385 °C, the semi-solid structure contained larger solid particles, and a nonuniform liquid phase was obtained, as shown in Fig. 7d.

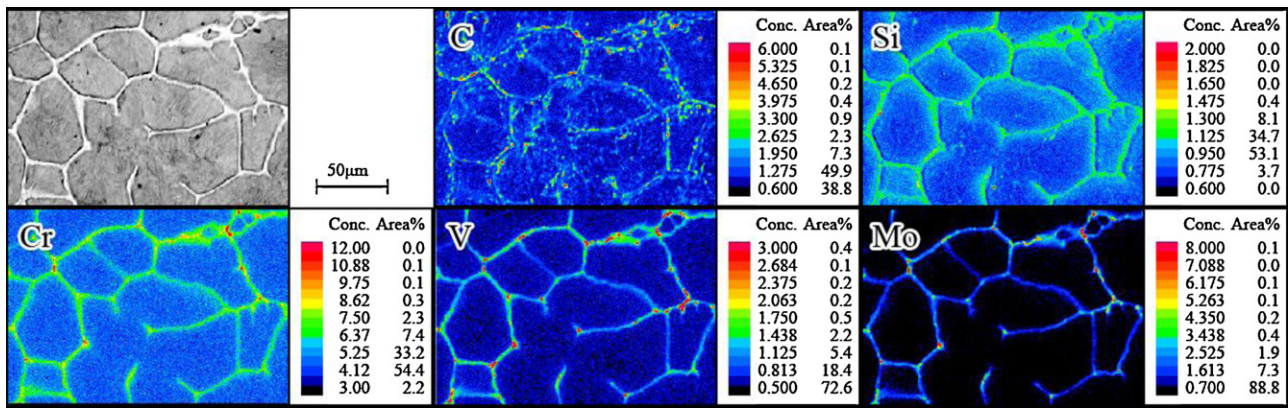


Fig. 6. SEM-EPMA mapping of RAP-processed cast Cr–V–Mo steel (predeformed with 50% height reduction).

### 3.4. Effects of heating strategy on microstructure

The microstructures of the 50% predeformed specimens heated at various heating rates (5, 20 and 50 °C/s) and quenched at various temperatures after 20 s isothermal holding are shown in Fig. 8. When the heating rate is 50 °C/s, the grain size of the specimens at 1250 °C and 1385 °C is about 30 µm and smaller than those of specimen heated at a heating rate of 5 °C. These discrepancies in grain size were attributed to the effects of the heating rate on the recrystallization and growth of austenite grains. According to the work by Muljono et al. (2001), the degree of nucleation increases in the initial stage of recrystallization as the heating rate increases.

Alogab et al. (2007) suggested that the population of small austenite grains increases with increasing heating rate. When heating rate is higher, the grains of one-phase austenite structure are smaller, as shown in Fig. 8a. As partial melting mainly occurred at grain boundaries, the finer austenite structure transforms to a finer semi-solid structure at 1385 °C shown in Fig. 8c. The lower heating rate leads to fewer number of recrystallized grains and provides a longer time for the growth of grains with further heating. A coarse microstructure is exhibited by the RAP-processed specimen heated at a lower heating rate.

Two groups of experiments were carried out, to investigate the effects of holding time during partial melting. In the first group, a

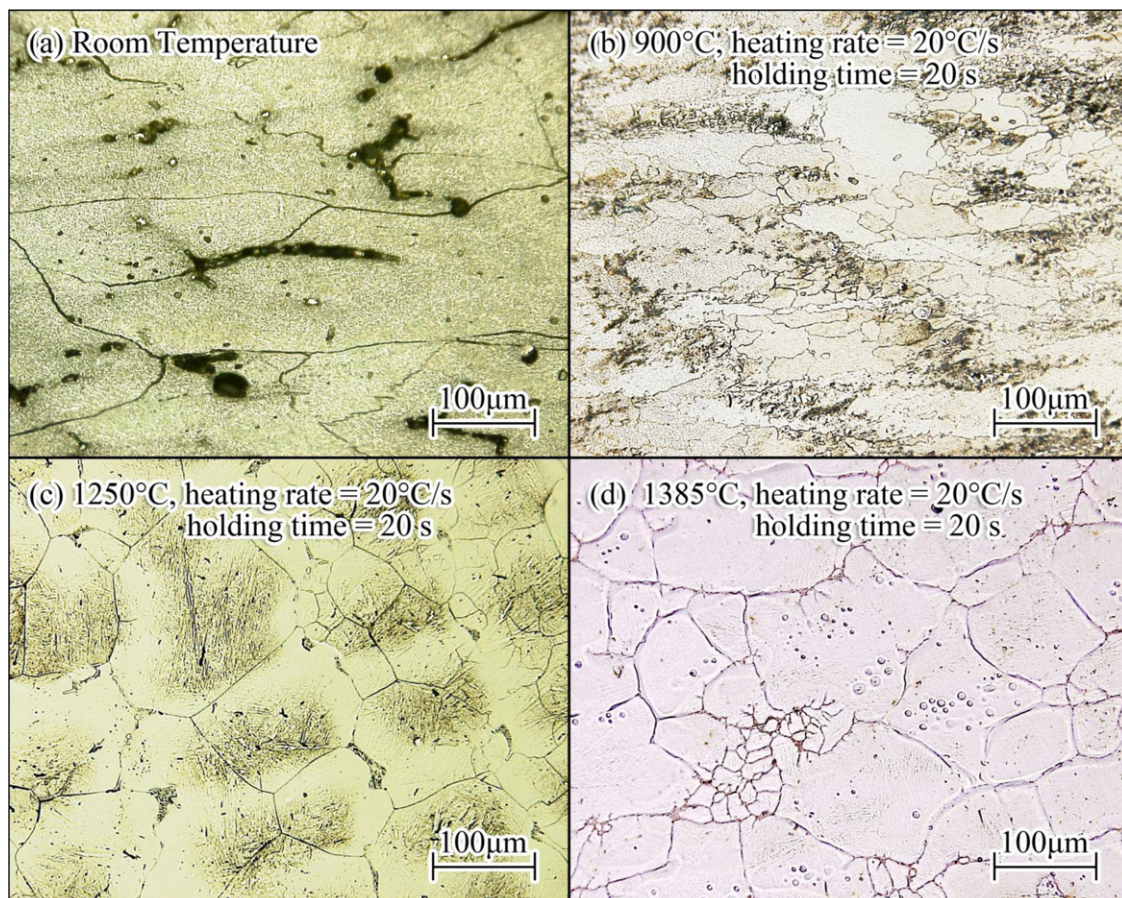


Fig. 7. Optical micrographs of specimen compressed at 300 °C with 25% height reduction and quenched from various temperatures after 20 s isothermal holding.

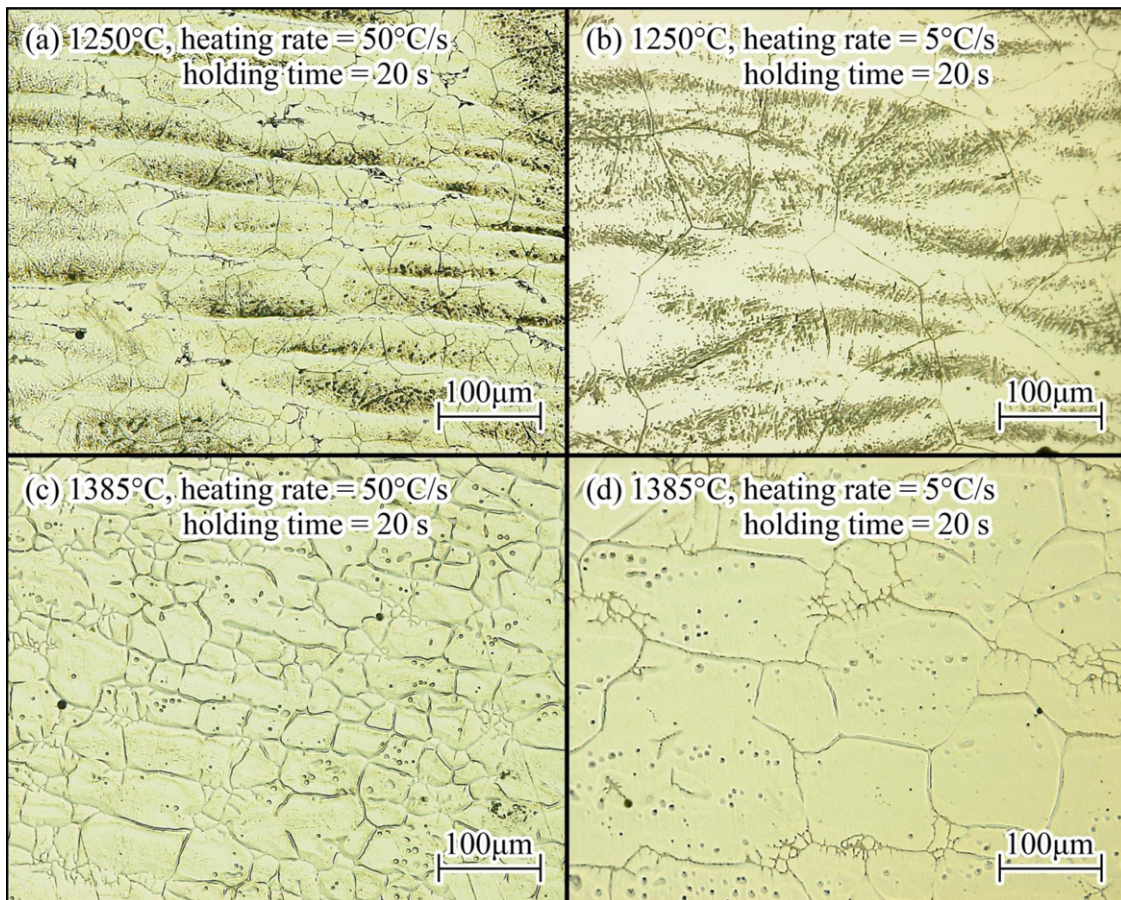


Fig. 8. Microstructures of predeformed specimens partially melted at different heating rates and quenched at different temperatures.

50% predeformed cast specimen was heated to 1385 °C at 50 °C/s and isothermally held for 100 or 300 s. In the second group, the specimens were heated to 1250 °C at the same heating rate and held for 100 or 300 s isothermally, then heated to 1385 °C, and held for 20 s isothermally. Fig. 9 shows two typical quenched microstructures of such specimens. In the specimen held for 300 s at 1385 °C, the liquid films were thicker and the liquid drops were fewer and larger. According to Püttgen et al. (2005), ripening driven by interfacial energy occurs during prolonged isothermal holding and leads to the combination of solid particles and the coarsening

of the liquid phase, hence increasing the size of solid particles but decreasing their number.

The specimen shown in Fig. 9b showed that the long holding time at 1250 °C also leads to a coarse semi-solid structure. The prolonged holding time during the grain growth stage causes the excessive growth of austenite grains and reduces the number of austenite grains. In further heating, the partial melting of the coarse austenite structure results in a coarse semi-solid structure. As the holding time at 1385 °C is only 20 s, the entrapped liquid drops in Fig. 9b are more discrete than those in Fig. 9a.

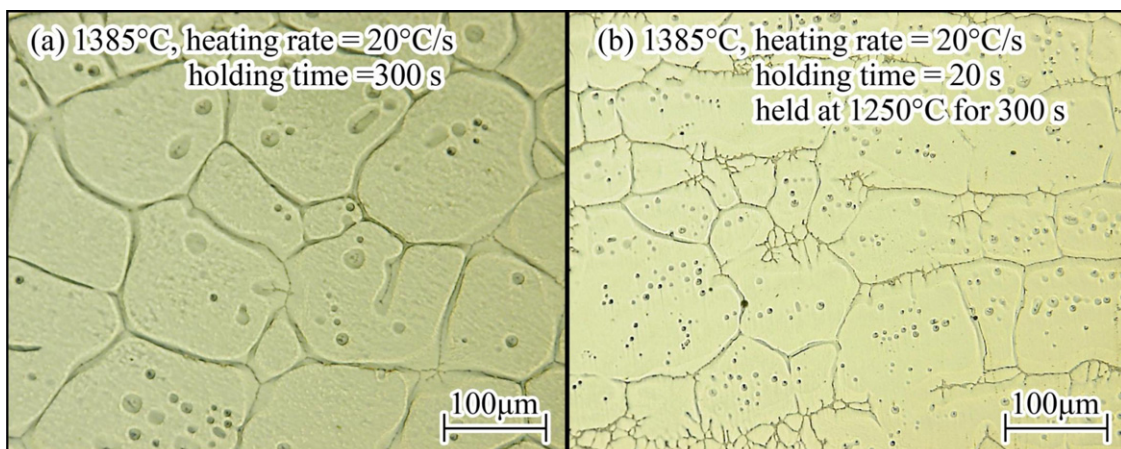
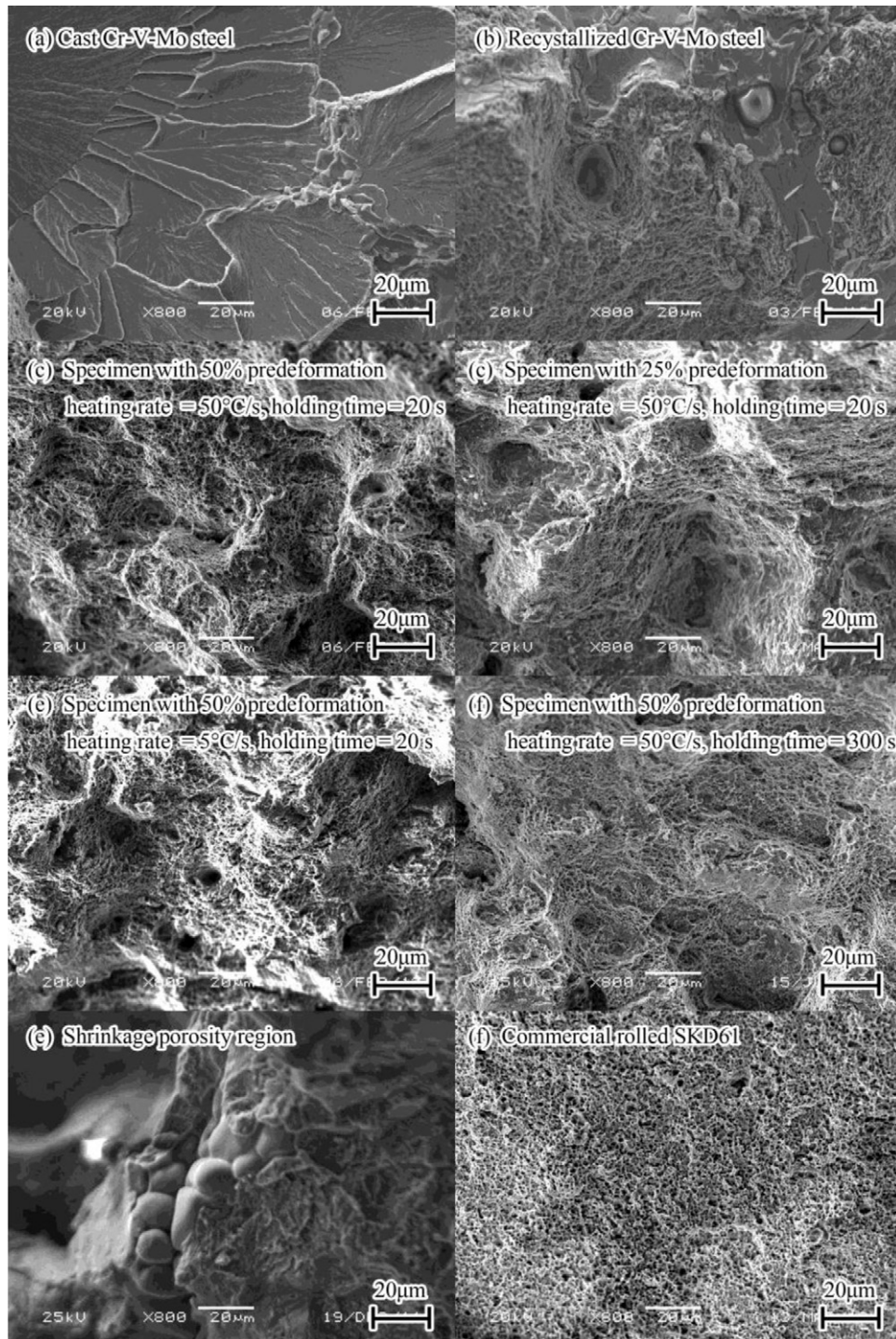


Fig. 9. Microstructures of cast Cr-V-Mo steel specimens RAP-processed using different heating strategies.

**Table 2**  
Effects of various processing conditions on yield strength, ultimate strength, and elongation of cast Cr–V–Mo steel (mean of five tests).

Processing condition	Yield strength (MPa)	Ultimate strength (MPa)	Elongation (%)
Cast	145 ± 20	398 ± 30	2.2 ± 0.5
50% predeformed; recrystallized	436 ± 10	556 ± 20	9.6 ± 1.5
RAP with 50% predeformation and 50 °C/s heating rate and 20 s holding	432 ± 20	585 ± 30	17.5 ± 1.0
RAP with 25% predeformation and 50 °C/s heating rate and 20 s holding	284 ± 20	506 ± 30	7.8 ± 1.5
RAP with 50% predeformation and 20 °C/s heating rate and 20 s holding	430 ± 10	564 ± 20	12.8 ± 0.5
RAP with 50% predeformation and 5 °C/s heating rate and 20 s holding	428 ± 20	532 ± 30	10.4 ± 1.0
RAP with 50% predeformation and 50 °C/s heating rate and 300 s holding	315 ± 20	518 ± 30	5.6 ± 1.5
Commercial SKD61 steel (rolled)	302 ± 10	574 ± 10	30.5 ± 0.5



**Fig. 10.** SEM micrographs of fracture surfaces of specimens processed under various conditions.

#### 4. Mechanical properties

The yield strengths, ultimate strengths, and elongations of the specimens processed under various experimental conditions are shown in Table 2. The cast Cr–V–Mo steel exhibits poor mechanical properties. After recrystallization, the tensile strength of the specimen increases, but the improvement in elongation is not significant. Subsequent semi-solid processing improves tensile strength to 585 MPa and improves elongation to 17.5% (about twice that of the starting material). When the height reduction of predeformation is 25%, both tensile strength and elongation turn out to be low. A lower heating rate and a longer holding time in the partial melting stage lead to poor mechanical properties of RAP-processed specimens.

The fracture surfaces of the specimens are shown in Fig. 10. The large cleavage planes shown in Fig. 10a indicate that the cast specimen fails in the cleavage fracture mode. This result confirms the poor strength and toughness of it indicated by measurements. As both dimples and cleavage planes are observed on the same fracture surface of the recrystallized specimen (Fig. 10b), the fracture is identified as a mixed fracture mode. It is presumed that recrystallization refines the microstructure, leading to even finer grains and discrete carbides. The small dimples and improved strength are attributed to the refined structure. As shown in Fig. 10b, cleavage planes coexist with carbides. As discussed in Section 3.2, carbides do not dissolve completely during recrystallization, and some of them are located at grain boundaries. The existence of these carbides results in the specimens having poor plasticity and high brittleness. The fracture surfaces of the RAP-processed specimens with 50% predeformation and the commercial rolled SKD61 specimen mainly exhibit dimple fracture morphology, indicating a ductile fracture mode. In contrast to the relatively neat fracture surface of the rolled SKD61 specimen shown in Fig. 10h, the fracture surfaces of the RAP-processed specimens exhibit undulating shapes with several larger dimples, as shown in Figs. 10c–f. At the bottom of the larger dimples, small cleavage planes are observed. Such cleavage planes result from some undissolved carbides, causing the lower elongation of the RAP-processed specimens. The RAP-processed specimens predeformed with a smaller reduction or partially melted at a lower heating rate exhibit even coarser microstructure. These imperfect microstructures result in the fracture surface having larger cleavage planes at larger dimples bottoms and fractures. The existence of such large cleavage planes and fractures confirms the poor mechanical properties of these specimens. The shrinkage porosity shown in Fig. 10g causes the poor elongation of the specimen with 300 s isothermal holding time. According to Omar et al. (2004), shrinkage porosities are caused by the draining or solidification of thick liquid films during rapid cooling. Chayong et al. (2005) suggested that shrinkage porosities should be alleviated to achieve the ideal properties.

#### 5. Conclusions

The work conducted has demonstrated the potential of RAP to realize the manufacturing of tool steel products with less energy and time consumption. The main results are summarized as follows:

1. Recrystallization, austenitization, and partial melting occur in RAP and transform the coarse structure of cast Cr–V–Mo steel to finer spherical structure with a more homogeneous distribution of carbides.

2. Larger predeformation retains more energy in the predeformed specimen and causes sufficient recrystallization of the cast structure and dissolution of alloying element in further heating.
3. Higher heating rate and shorter holding time increases the degree of nucleation in recrystallization, inhibit the growth of austenite grains and the coarsening of solid particles.
4. Larger predeformation (50%), higher heating rate (50 °C/s), and shorter holding time (20 s) in RAP can refine the microstructure and improve strength and elongation more effectively.

#### Acknowledgment

This study was financially supported by a Grant-in-Aid for Scientific Research on Innovative Area, “Bulk Nanostructured Metals”, through MEXT, Japan (contract No. 22102005).

#### References

- Adachi, M., Sasaki, H., Harada, Y., Sakamoto, T., Sato, S., Yoshida, A., 1996. Method and apparatus for shaping semisolid metals. European Patent, 0745694A1.
- Alogab, K.A., Matlock, D.K., Speer, J.G., Kleebe, H.J., 2007. The effect of heating rate on austenite grain growth in a Ti-modified SAE 8620 steel with controlled niobium addition. *ISIJ International* 47, 1034–1041.
- Atkinson, H., Rassili, A., 2010. In: Atkinson, H., Rassili, A. (Eds.), *Thixoforming Steel*. Shaker Verlag, Aachen, Germany, pp. 13–18.
- Barani, A.A., Li, F., Romano, P., Ponge, D., Raabe, D., 2006. Design of high-strength steels by microalloying and thermomechanical treatment. *Materials Science and Engineering A* 463, 138–146.
- Chayong, S., Atkinson, H.V., Kapranos, P., 2005. Thixoforming of 7075 aluminum alloys. *Materials Science and Engineering A* 390, 3–12.
- Flemings, M.C., 1991. Behavior of metal alloys in the semisolid state. *Metallurgical Transactions* 22A, 957–981.
- Griffiths, W.D., McCartney, D.G., 1996. The effect of electromagnetic stirring during solidification on the structure of Al–Si alloys. *Materials Science and Engineering A* 216, 47–60.
- Haga, T., Kouda, T., Motoyama, H., Inoue, N., Suzuki, S., 1998. High speed roll caster for aluminium alloy strip. In: *Proc ICAA7. Aluminium Alloys: Their Physical and Mechanical Properties*, Charlottesville, VA, United States. *Trans. Tech. Publications*, pp. 327–332, 2000.
- Hirt, G., Shimahara, H., Seidl, I., Kuthe, F., Abel, D., Schonbohm, A., 2005. Semi-solid forging of 100Cr6 and X210CrW12 steel. *CIRP Annals – Manufacturing Technology* 54, 257–260.
- Kirkwood, D.H., Sellars, C.M., Eliasboyed, L.G., 1991. Fine grained metal composition. US Patent, 5,037,498.
- Li, J., Sugiyama, S., Yanagimoto, J., 2005. Microstructural evolution and flow stress of semi-solid type 304 stainless steel. *Journal of Materials Processing Technology* 161, 396–406.
- Li, J., Sugiyama, S., Yanagimoto, J., Chen, Y., Guan, W., 2008. Effect of inverse peritectic reaction on microstructural spheroidization in semi-solid state. *Journal of Materials Processing Technology* 208, 165–170.
- Metals Handbook, 1998. *Metals Handbook*, vol. 15., 9th ed. ASM International, OH, pp. 306–314.
- Meng, Y., Sugiyama, S., Yanagimoto, J., 2012. Microstructural evolution during RAP process and deformation behavior of semi-solid SKD61 tool steel. *Journal of Materials Processing Technology* 212, 1731–1741.
- Muljono, D., Ferry, M., Dunne, D.P., 2001. Influence of heating rate on anisothermal recrystallization in low and ultra-low carbon steel. *Materials Science and Engineering A* 303, 90–99.
- Omar, M.Z., Atkinson, H.V., Palmiere, E.J., Howe, A.A., Kapranos, P., 2004. Microstructural development of HP9/4/30 steel during partial remelting. *Steel Research International* 75, 552–560.
- Püttgen, W., Bleck, W., Seidl, I., Kopp, R., Bertrand, C., 2005. Thixoforged damper brackets made of the steel grades HS6-5-3 and 100Cr6. *Advanced Engineering Materials* 7, 726–735.
- Püttgen, W., Hallstedt, B., Bleck, W., Uggowitzer, P.J., 2007. On the microstructure formation in chromium steels rapidly cooled from the semi-solid state. *Acta Materialia* 55, 1033–1042.
- Roberts, G., Krauss, G., Kennedy, R., 1998. *Tool steels*, 5th ed. ASM International, OH, pp. 67–97.
- Song, R., Kang, Y., Zhao, A., 2008. Semi-solid rolling process of steel strips. *Journal of Materials Processing Technology* 198, 291–299.
- Spencer, D.B., Mehrabian, R., Flemings, M.C., 1972. Rheological behavior of Sn–15 Pct Pb in the crystallization range. *Metallurgical Transactions* 3, 1925–1932.
- Young, K.P., Kyonka, C.P., Courtois, J.A., 1983. Fine grained metal composition. US Patent, 4,415,374.